Novel Common-Differential Inductance Coils With Dual Signal Conditionings for Separation of Lift-Off and Defects

Qiping Ma, Guiyun Tian, *Senior Member, IEEE*, Bin Gao, *Senior Member, IEEE*, Mark Robinson, Changrong Yang, and Emmanuel Tashiwa Ibrahim

***Abstract*—Lift-off has a significant impact on defect discrimination and qualification. Estimating lift-off and evaluating defects is a critical issue for eddy current testing (ECT). In this article, a novel sensor that separates lift-off and defects is proposed. This uses common- and differential-mode coils with a dual signal conditioning circuit. Specifically, it comprises two hollow rectangular excitation coils located on the first and third layers of the printed circuit board (PCB), serving as the two arms of an ac bridge circuit. The output from the bridge signal is used for lift-off estimation since the coaxial configuration and small coil fill ratio make it specifically sensitive to lift-off variation. The other pair of rectangular receiver coils are situated on the second and third layers and placed in the middle of the hollow transmitter. This forms a transformer with excitation coils and is only sensitive to defects. The signals from these two complementary outputs allow lift-off to be used as auxiliary information for defect discrimination. Simulations and experiments were carried out to validate the method. This proves that a combination of coil configurations with different signal conditioning techniques can be employed for separating multiple parameters.**

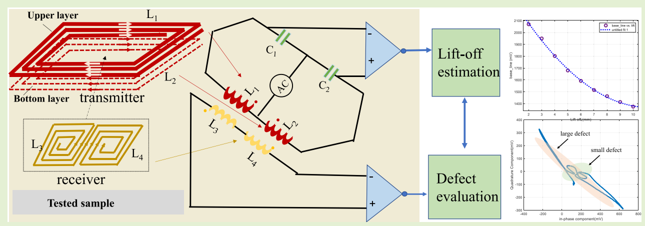

***Index Terms*—Bridge, defect detection, differential transformer, eddy current testing (ECT), lift-off.**

I. Introduction

EDDY current testing (ECT) is an attractive technique for ensuring the safety and maintenance of energy production, transportation, or other infrastructures. It is noncontact and sensitivity to multiple parameters such as conductivity and magnetic permeability [1]. Compared to ultrasonic testing (UT) and electromagnetic acoustic transducer (EMAT) methods, it has the advantages of not requiring coupling and requiring conversion efficiency [2], [3]. It is preferred over magnetic flux leakage (MFL) as it does not require a strong magnetization device [4]. However, the challenging issue for ECT is that it is easily perturbed by disturbances such as lift-off, vibration, and inclusion [5]. Under these circumstances, useful information associated with the specimen can be masked and lead to sensitivity or recognition accuracy reduction [6]. To address these issues, ECT probes are a possible solution to assess the reliability and accuracy of detection [7]. Thus, research on lift-off measurement and estimation and defect detection has attracted extensive attention.

Currently, studies related to lift-off and defect detection can be summarized [8] into the following:

1) response characteristics and theoretical analytical modeling;
2) probes' design and optimization;
3) features with frequencies and signal processing methods.

Among these, the design and realization of the probes' structure are crucial for improving the performance of detection as their optimization directly depends on the principle of the physical field and significantly affects the quality of the signal to be processed. The shape of coils, probe configuration, and operation mode have a significant influence [9]. For instance, rectangular or square-shaped coils have a better ability to minimize the impact of lift-off [10]. Probe configurations generally refer to the way one coil or more coils are arranged to achieve the best coupling with the region of interest for detection [11]. The mode of operation

Manuscript received 19 October 2023; accepted 20 November 2023. Date of publication 6 December 2023; date of current version 12 January 2024. This work was supported in part by the Department of Science and Technology of Sichuan Province under Grant 2021JDTD0030, in part by the National Natural Science Foundation of China under Grant 62103082, and in part by the China Scholarship Council under Grant 202206070055. The associate editor coordinating the review of this article and approving it for publication was Dr. Ponnalagu R. N. *(Corresponding author: Guiyun Tian.)*

Qiping Ma and Guiyun Tian are with the School of Automation Engineering, University of Electronic Science and Technology of China, Chengdu 611731, China, and also with the School of Engineering, Newcastle University, NE1 7RU Newcastle upon Tyne, U.K. (e-mail: mqp@std.uestc.edu.cn; g.y.tian@newcastle.ac.uk).

Bin Gao is with the School of Automation Engineering, University of Electronic Science and Technology of China, Chengdu 611731, China (e-mail: bin_gao@uestc.edu.cn).

Mark Robinson, Changrong Yang, and Emmanuel Tashiwa Ibrahim are with the School of Engineering, Newcastle University, NE1 7RU Newcastle upon Tyne, U.K. (e-mail: c.yang1@newcastle.ac.uk; mark.robinson@newcastle.ac.uk; e.t.ibrahim2@newcastle.ac.uk).

Digital Object Identifier 10.1109/JSEN.2023.3336066

relates to how coils are wired and interface with the subsequent measuring equipment. They are generally classified into four categories: absolute, differential, reflection, and hybrid [12]. Absolute-type probes generally consist of a single coil that generates eddy currents and senses changes in the eddy current field [13]. This common-mode probe is sensitive to common-mode factors such as lift-off and temperature. Thus, it is usually used for displacement measurement, but it needs to minimize these effects for defect detection. A differential probe typically utilizes two coils wound in opposite directions [14]. The output signal in differential mode directly reveals the different components of the background signal [15]. The reflection probe typically consists of two coils, with one serving as a transmitter to generate eddy currents and the other one serving as a receiver coil to detect changes in the material [16]. The individual optimization of these two coils for specific purposes is a characteristic advantage of this type of probe. A hybrid configuration of the probe can be any combination of the previously described designs, tailored for sensitivity enhancement or multiparameter measurement. Based on the characteristics of these different types of configurations, numerous structures have been proposed for lift-off suppression and defect detection. For example, a circular exciting coil with a rectangular tangential pickup coil placed at the center of the former one was presented in [17], and in this design, the output signal only reflects the disturbed eddy current flows along the pickup coil because the axis-symmetrical lift-off noise has no influence on the pickup one. A similar concept, with an orthogonal axial eddy current probe, was introduced to detect the uneven surface of weld defects on carbon-steel plate [18]. A double-layer differential probe was designed for producing a symmetrical primary magnetic field that reduces lift-off interference and can achieve higher lift-off detection [19]. A U-shape magnetic core and magnetic field signal were used to study the effect of the lift-off invariant point [20]. A differential eight-shaped transformer fabricated through flexible printed circuit board (PCB) technology was employed for rolling contact fatigue cracks with different orientations. It showed that this type of probe can suppress lift-off effects during detection [21].

Although there are many approaches to mitigate lift-off interference, accurately qualifying and distinguishing them from multiple interferences remains challenging. Many studies consider lift-off in combination with multiple features and multimode measurement and this is likely to be a trend in future research. For example, differential changes in magnetic flux were utilized to obtain lift-off information in a pulsed eddy current (PEC), using the features acquired from the detection and reference signals [22]. A triple-coil sensor, which operates as two coil pairs and works simultaneously in a multifrequency mode, was investigated [23]. Through analyzing the differences in peak frequencies, the impact of lift-off effects can be reduced. A noncoaxial transmitter-receiver sensor with the feature of conductivity point of intersection was investigated in PEC testing . With this feature, the lift-off and thickness of the specimen can be determined [24]. To enable a broader range of lift-off detection, dual frequencies were applied in a high working frequency system. The lift-off was reconstructed from the linear relationship between lift-off and ratio of eddy current signals [25]. A probe based on an LC resonator was employed, and a resistance–frequency plane was established to eliminate lift-off effects and to demonstrate electrical conductivity [26]. Different sensors' signal conditioning and digital interfaces were reviewed () [27]. Subsequently, a method for measuring lift-off distance and determining defects using an inductance to digital converter (LDC) chip was presented. This demonstrates that different signal conditioning circuits can yield varying measurement parameters. Another solution for lift-off and defect measurement involves realizing distributed capacitance variation as a function of lift-off in PEC. In this way, lift-off was determined through leakage current measurement while simultaneously achieving defect detection [28]. Subsequently, a configuration comprising one transmitter and two different receiver coils was provided in [29]. In this configuration, the larger coil was used for lift-off measurement and the smaller one was used for defect detection. In addition, the relationship between signal conditioning and various parameter measurements has garnered attention in recent years. A composite structure combining both induction and capacitance was constructed, allowing for dual-mode simultaneous detection and qualification of defects [30]. However, the modulation/demodulation process with pulse/multifrequency and coil configuration designs with multimode is complex. This article is based on our previous research to solve problems using dual signal conditioning during pipeline inspection to provide multiparameter measurement. Simple systems and designs are targeted.

TABLE I
COMPARISON WITH PREVIOUS WORK

Parameters	Previous work	This paper
Signal conditionings circuit	AC bridge +transformer	AC bridge +transformer
Coil configuration	Side by Side	Vertical placement
Method	Multiple parameters fusion	Multiple parameters separation
Application stage	Defect detection process	Assisted defect quantification process
Purpose	Lift-off suppression for sensitivity improvement	Lift-off and defects separation

Comparing our previous work and our current study [31], they differ in terms of coil structure and applications (as shown in Table I). In our previous work, the focus was on reduced detection sensitivity due to lift-off during defect detection. It employed a dual-differential probe design and utilized a multiparameter fusion approach to suppress the lift-off effect and enhance detection sensitivity. In contrast, the current study aims at the quantification of defects. It utilizes a common-mode excitation coil structure to separate lift-off, aiding defect discrimination and quantification. It indicates that multiparameter measurement and separation for different applications can be achieved through different configurations and signal conditions.

This article is organized as follows. Section II presents a theoretical derivation based on the equivalent circuit model for the relationship between the output voltage from two signal conditions with lift-off as well as defects. Section III presents the simulation results that validate the proposed method. The

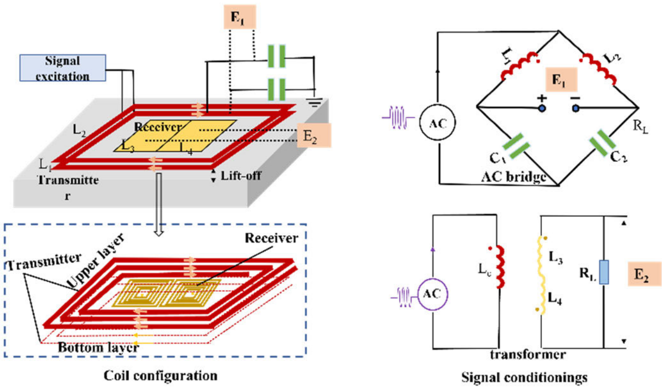

Fig. 1. Proposed system diagram.

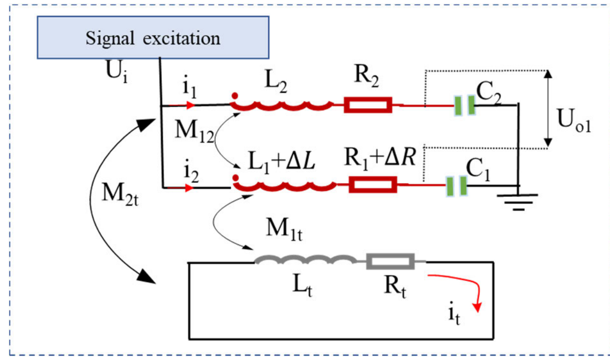

Fig. 2. Equivalent circuit model for bridge.

experiments conducted with different types of defects on #45 steel and X80 carbon steel for lift-off and defect separation are discussed in Section IV. The conclusion and future work are demonstrated in Section V.

II. Principle of the Proposed Method

Based on the platform with two signal conditions proposed in the previous study [32], a diagram for a new method with a novel coil configuration design is shown in Fig. 1. The red spiral rectangular coils serve as the common-mode coil in the system. They are positioned on the first and third layers of the PCB and have a unique design with a small coil fill ratio, as the center of the coil hollow. These coils are connected in series with capacitances, effectively forming the arms of the bridge circuit [33]. Their main function is to act as transmitters, generating the primary magnetic field during the ECT process. After the interaction of the transmitter, eddy currents are generated on the sample, and the eddy currents produce a secondary magnetic field, which is captured by the differential receiver represented by the yellow line coils. The arrangement of the receiver coils and the transmitter coils effectively forms a differential transformer. The differential transformer setup helps significantly in enhancing the sensitivity and accuracy of the ECT system. The output signals from both the bridge circuit and the differential transformer are sent to the differential amplifier and then provide crucial data for further analysis and evaluation. The details of the technique and the relationship between lift-off and defect detection based on the equivalent circuit model are further elaborated in this article. This approach aids in accurately assessing lift-off and detecting defects during ECT, making it valuable for nondestructive evaluation applications.

A. Common-Mode Transmitter and Bridge Circuit for Lift-Off Measurement

The equivalent circuit based on common-mode transmitter and bridge circuit signal conditioning circuit is shown in Fig. 2. A constant frequency and voltage sine wave is produced by the signal generator, and this is fed into a power amplifier to enhance the current-driving ability of the transmitter. The ac excitation source U_1 is amplified by the power amplifier and is injected into the two coils. The direction of current in the two coils is the same. The primary magnetic field produced under the excitation interacts with the test sample. The magnetic field produced by these two coils is superimposed on each other, creating a coil-like configuration with two layers. An eddy current is then induced on the sample, generating a secondary magnetic field that influences the impedance of the transmitter coils. The coils L_1 and L_2 can be regarded as the arms of a bridge circuit. The difference in output amplitude between two capacitances' signal is connected to a differential amplifier to amplify the strength. L_1 and L_2 have the same dimensions and linewidth, resulting in similar inductance and resistance, i.e., $L_1 \approx L_2$ and $R_1 \approx R_2$. The arm capacitance has a constant value, which is approximately $C_1 \approx C_2 \approx C_s$. The equivalent inductance and resistance of the induced eddy current are represented as L_t and R_t, respectively. The mutual inductance between the sample and two coils as well as the mutual inductance between two coils are denoted as M_{1t}, M_{2t}, and M_{12}. The current flowing through coils L_1 and L_2 is represented as i_1 and i_2, respectively. The short current induced on the sample is denoted as i_t. Under this configuration, the system behaves similar to a displacement sensor [34]. We explore the relationship between output amplitude and lift-off employing an equivalent circuit model based on Kirchhoff laws. The common component ($M_{12} = M_{21}$) when passing through the differential amplifier was canceled out. Therefore, we choose to ignore the mutual inductance between L_1 and L_2 in this model

$$\begin{cases} R_i i_i + j\omega L_i i_i + \dfrac{1}{j\omega C_s} i_i - j\omega M_{it} i_t = U_1 \\ R_t i_t + j\omega L_t i_t - j\omega M_{it} i_i = 0 \end{cases} \tag{1}$$

where $i = 1, 2$, ω is the angular frequency of the excitation signal, which is $\omega = 2\pi f$, and R_i presents the series resistance of the transmitters. The mutual inductance M_{it} between coils and the tested sample can be expressed using the coupling coefficient k_{it}, which solely depends on the lift-off x. This is because the geometric parameters of coils remain constant

$$M_{it} = k_{it}(x)\sqrt{L_i L_t}\;(0 < k < 1). \tag{2}$$

From (1), we can derive

$$i_i = \frac{U_1}{R_i + \frac{(\omega M_{it})^2 R_t}{R_t^2 + (\omega L_t)^2} + j\omega\left(L_i - \frac{(\omega M_{it})^2 L_t}{R_t^2 + (\omega L_t)^2} + \frac{1}{C_s}\right)}. \tag{3}$$

Hence, the equivalent impedance becomes

$$Z_i = R_i + \frac{(\omega M_{it})^2 R_t}{R_t^2 + (\omega L_t)^2} + j\omega\left(L_i - \frac{(\omega M_{it})^2 L_t}{R_t^2 + (\omega L_t)^2} + \frac{1}{C_s}\right). \tag{4}$$

Then, the equivalent inductance R_i' and resistance L_i' are given by

$$\begin{cases} R_i' = R_i + \dfrac{(\omega M_{it})^2 R_t}{R_t^2 + (\omega L_t)^2} = R_i + \Delta R_i \\ L_i' = L_i - \dfrac{(\omega M_{it})^2 L_t}{R_t^2 + (\omega L_t)^2} = L_i - \Delta L_i. \end{cases} \tag{5}$$

Lift-off directly impacts the intensity of eddy current induced on the sample, subsequently causing a change in impedance and leading to a variation in the current. The measured voltage is obtained as the voltage difference across the capacitance, and it can be described as follows:

$$\Delta U_{o1} = \frac{1}{j\omega C_s}\Delta i_1 - \frac{1}{j\omega C_s}\Delta i_2. \tag{6}$$

Due to the parallel connection of the branch containing i_1 and the branch containing i_2, we have the following equations:

$$\Delta i_i \Delta Z_i = U_1 - \frac{1}{j\omega C_s}\Delta i_1. \tag{7}$$

Therefore, Δi_i is inversely proportional to ΔZ_i

$$\Delta i_i = \frac{U_1}{\Delta Z_i + \frac{1}{j\omega C_s}} \propto \frac{1}{\Delta Z_i}. \tag{8}$$

When the lift-off is increased, the current ΔI_1 will decrease because L_1 is closer to the surface of the specimen and generates a stronger eddy current, leading to a greater change in impedance ΔZ_1. Due to the parallel connection of L_1 and L_2, the increase in Δi_1 will cause a decrease in Δi_2. Consequently, the change of output ΔU_{o1} can be simplified as follows:

$$\Delta U_{o1} \propto \frac{\Delta i_1}{j\omega C_s} \propto \frac{1}{\Delta Z_1} \propto \frac{1}{F(x)} \tag{9}$$

$$\Delta Z_1 = F(x) = \Delta R(x, \sigma, \mu, f) + \Delta L(x, \sigma, \mu, f) \tag{10}$$

where $F(x)$ is a function related to the lift-off, implying that lift-off value can be determined from the measured voltage. This approach allows for the reduction of other common influences, such as temperature variation [33].

B. Differential Transformer for Defect Measurement

A pair of differential rectangular PCB coils L_3 and L_4 are in the middle hollow of transmitter coils. The coils are wound in opposite direction and pick up defect information from the eddy current. Since the two coils of the transmitter have the same direction of current, they generate a total magnetic field. We simplified these coils as a whole self-inductance coil L_c and internal resistance R_c. Suppose that the total self-inductance and internal resistance of the differential receiver are L_d and R_d, respectively. Under this configuration, the transmitter and receiver coil form the transformer signal condition. The magnetic field generated by the transmitter and eddy current was induced on the sample. From Lenz's law, the direction of the secondary magnetic field produced by eddy current is opposite to the primary magnetic field. Defects perturb the eddy current, causing changes in the magnetic flux density and the inductive electromotive force (EMF) in the receiver. The equivalent transformer model is shown in Fig. 3. The time-varying primary magnetic flux couples with the receiver directly and indirectly via the sample. Assume that the current flowing into the transmitter and receiver is i_1 and i_3. R_L is the load resistance. Based on the transformer circuit model, the following equations can be deduced (11), as shown at the bottom of the next page, where U_i is the excitation voltage. E_1 and E_2 are the mutually induced EMF between transmitter and receiver. Mc_0 is the direct mutual inductance between transmitter and receiver. Mc_1 is the mutual inductance of transmitter and receiver through the sample. s_1 and s_2 can be regarded as self-coupling of transmitter and receiver through the sample. Δr_c and Δr_d are the changes of internal resistance affected by the sample. Then, we can obtain the output voltage of receiver U_{o2}

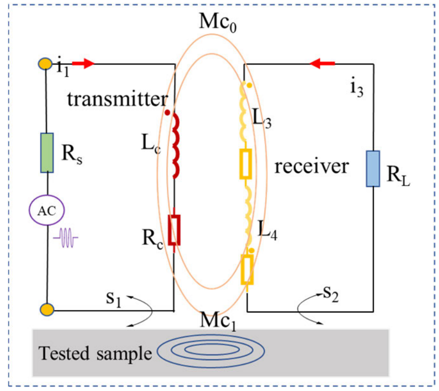

Fig. 3. Equivalent circuit model for the differential transformer.

$$U_{o2} = j\omega (L_d + Mc_1 + s_2) i_3 + (R_d + \Delta r_d) i_3 - Mc_0) i_1. \tag{12}$$

If there is a defect, then the coupling between the specimen and the probe would be changed, causing the impedance on receiver $(Mc_1 + s_2 + \Delta r_d)$ to change as well. The indirect mutual inductance Mc_1 contains information for the sample. Thereby, this configuration can be used for defect measurement.

In addition, the main sources of background noise from the self-inductance of the receiver coil and mutual inductance (Mc_0) between the transmitter and receiver coils limit the SNR of the response of detection signal. The background noise and lift-off caused by the self-inductance of the pickup coil can be eliminated by differential structure.

III. Simulation Setup and Multiparameters Estimation

To validate the proposed method, a finite element model (FEM) simulation was set up with an ac/dc module and circuit module to analyze the electromagnetic field in COMSOL Multiphysics version 6.0. In this section, the influence of the

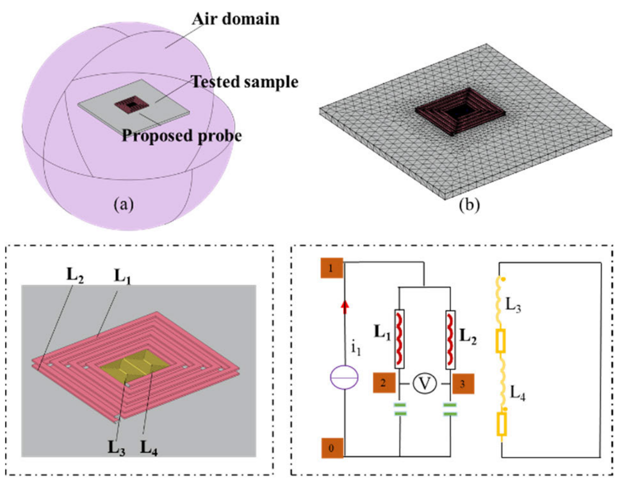

Fig. 4. Simulation configuration. (a) 3-D model set-up. (b) FEM mesh diagram. (c) Probe geometry. (d) Circuit interface.

coil configuration was first investigated. Then, the comparison of results for bridge and transformer for lift-off and defect was explored.

Fig. 4(a) shows a 3-D model of the coils and sample in a big air domain and Fig. 4(b) shows the finer mesh generation. Due to the double signal conditions, the circuit interface is used to couple coils and use a voltage meter to measure the voltage between the capacitances. The geometry of the coils is shown in Fig. 4(c). At the circuit interface, all the components link with others through nodes, as shown in Fig. 4(d). The excitation method of the transmitter is a circuit current. Thus, a constant current source, a voltage meter, and two external I versus U as well as two capacitances are used. The output of the voltage is the bridge output. As for differential receiver, we can make the current in the coil setting 0 A, and then, the software can couple the magnetic field with the transmitter. The output of the voltage can be determined directly through the derived value using the function of mf.Vcoil_x. To save time and reduce freedom of the calculation, a frequency-domain analysis was adopted for the ac/dc module. Parametric sweep is employed as well to investigate the different values of lift-off and response of scanned defects. The parameters of the simulation setting are shown in Table II.

A. Influence of the Coil Configuration

This article proposes a novel configuration with a hollow common-mode transmitter with bridge signal conditioning. The influence of two different coil fill ratios with hollow (small coil fill ratio) and solid (large coil fill ratio) shape on lift-off and defects detection are studied, as shown in Fig. 5. These two coils have the same dimensions and the same linewidth. According to the system described above, these two coils are analogous to a bridge circuit. We can determine the relationship between these two configurations and lift-off by moving the probe in a direction perpendicular to the surface of the specimen from 0 to 10 mm. After comparing the bridge output under these two configurations, we can see that the hollow coil and solid coil exhibit similar trends in lift-off shown in Fig. 6(a). Although the output voltage of a solid coil is slightly higher than that of a hollow coil, both types of coil configuration with bridge output amplitudes decrease with increasing lift-off. This is because as the lift-off increases, the coupling between the coil and the eddy current decreases, which is also consistent with (8) of theoretical analysis.

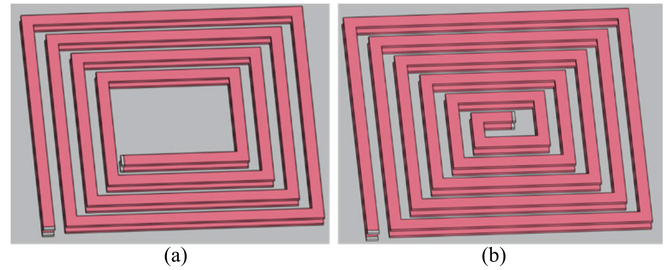

Fig. 5. Comparison of coil fill ratio. (a) Hollow. (b) Solid.

TABLE II
SIMULATION PARAMETERS

	Electrical conductivity	Relative permeability	Size/mm
transmitter	5.998e7[S/m]	1	80×60×0.5
Receiver/each	5.998e7[S/m]	1	28×20×0.5
Tested sample	5.5e6[S/m]	190	400×400×10
Air domain	1	1	r=400mm
Capacitance	0.87uF		

Subsequently, we investigated the influence of the configurations on defect detection. A 20 × 20 × 4 mm defect was made and Ampère's law was used to set the conductivity of the defect region as 0. Similarly, the amplitude output of voltage was obtained when the probe passed through the defect region. Fig. 6(b) shows the impact of the bridge circuit on defects in the context of a hollow coil design. The observed amplitude variations can be explained as follows. When there are no defects, the output voltage of the bridge corresponds to the difference in distance between the upper and lower hollow coils to the test specimen. However, when a defect is present, the change in amplitude reflects alterations in defect information. Amplitude variation is related to defect size, and larger defects cause greater disturbances. This shows that the solid configuration increases the output voltage and has better sensitivity to the defect. This is because a higher fill ratio

$$\begin{bmatrix} j\omega Mc_0 & j\omega Mc_1 \\ j\omega Mc_0 & j\omega Mc_1 \\ j\omega\left(L_c+s_1\right)+\left(R_1+\Delta r_c+R_s\right) & 0 \\ 0 & j\omega\left(L_d+s_2\right)+\left(R_d+\Delta r_d+R_s\right) \end{bmatrix} \begin{bmatrix} i_1 \\ i_3 \end{bmatrix} = \begin{bmatrix} E_1 \\ E_2 \\ j\omega\left(Mc_0+Mc_1\right)i_3+U_i \\ j\omega\left(Mc_0+Mc_1\right)i_1 \end{bmatrix} \quad (11)$$

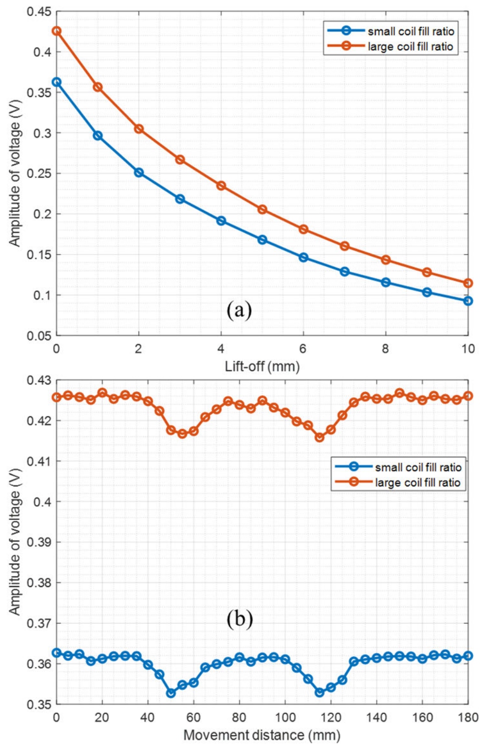

Fig. 6. (a) Lift-off response comparison of two coils fill ratio. (b) Defects measurement comparison of two coils fill ratio.

helps to maximize the interturn magnetic coupling in the coil winding and it increases magnetic field strength to coupling with defect. For our purpose, this coil is intended for lift-off measurement. It is expected to be sensitive only to lift-off. Therefore, we have employed a coil structure with a smaller fill factor, which is less sensitive to defect detection.

B. Bridge Signal Conditioning for Lift-Off Measurement and Transformer for Defects Measurement

Once the coil configuration is determined, the signal conditioning can be further investigated. We selected the hollow coil configuration and picked up the voltage from two signal conditioning circuits simultaneously and compared the performance of these two conditioning circuits under different lift-offs while scanning the same defect. The results are shown in Fig. 7(a). This shows that the output of the bridge significantly decays exponentially, while the output of the differential transformer changes slightly as the lift-off increases. This verifies that the bridge output is sensitive to lift-off variation. Fig. 7(b) shows the amplitude of dual signal conditioning circuits with the probe passing through the defect. It indicates that the differential transformer has higher sensitivity for defect detection, which verified the theoretical derivation in Section II.

In summary, the bridge output is more sensitive to lift-off and the differential transformer is more sensitive to defects. Therefore, these two complementary characteristics are achieved through using the relationship between coil structure and signal conditioning circuits. This design not only demonstrates the importance of considering both coil structure and the chosen conditioning circuit when designing sensors but also highlights the value of this research for future engineering applications in ECT. It can be used to separate lift-off, assisting in defect discrimination and quantification.

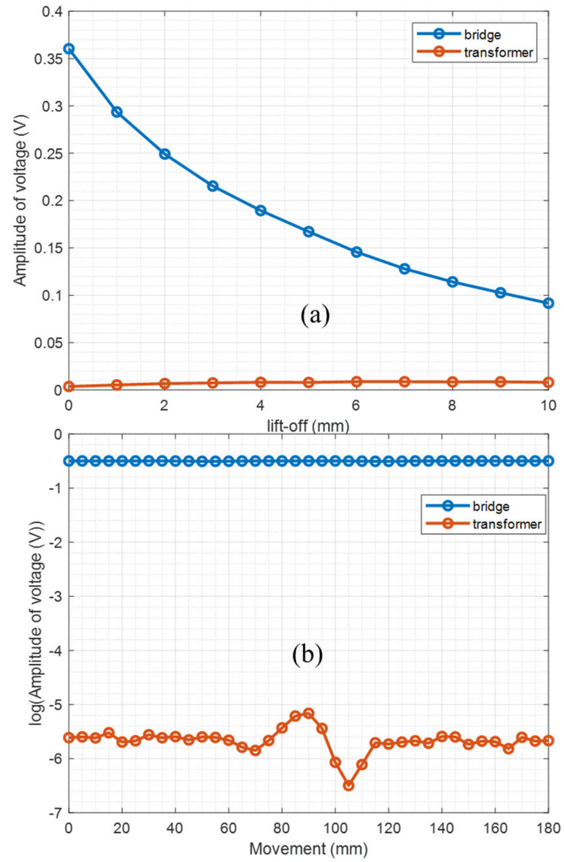

Fig. 7. (a) Comparison of the output of dual signal conditionings under lift-off variation. (b) Comparison of the output of dual signal conditionings for defects detection.

IV. Experimental Setup and Multiparameter Estimation

Based on the simulation findings several experimental designs were investigated to validate the common-differential mode with dual signal conditioning that has the complementary characteristics to detect lift-off and defects. Now, a combined solution method based on bridge and transformer method is proposed and employed for the separation of lift-off and defects. Finally, quantitative analysis and comparative analysis will be provided to demonstrate the advantages of the proposed method.

A. Experimental Setup and Sample Preparation

In this section, a prototype probe with the dual signal conditioning system was fabricated and used to validate the feasibility of the method. The diagram of the experimental setup is shown in Fig. 8(a). The integrated device includes a signal generator, power amplifier that was digitalized using an ADC chip, based on the system previously devised [31]. A 6-V sinusoidal waveform with a frequency of 400 kHz was injected into the power amplifier, and then, the signal was connected to the proposed multilayer PCB coil [as shown in Fig. 8(b)].

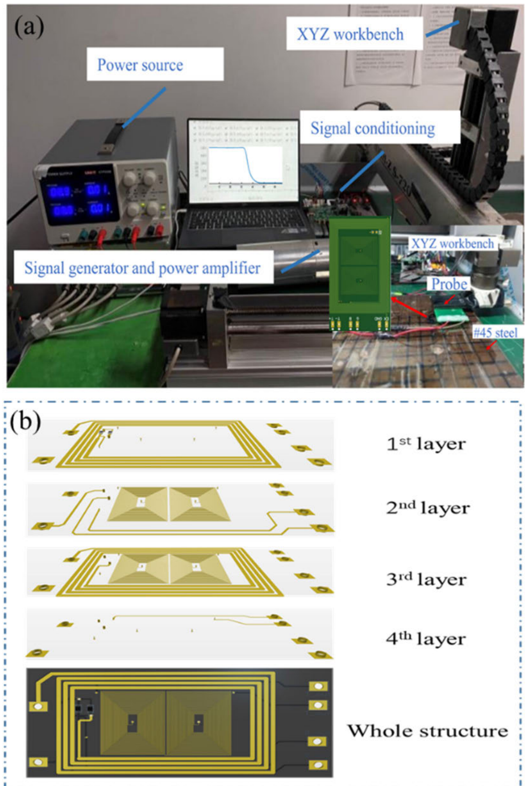

Fig. 8. (a) Experimental setup. (b) Detailed diagram of PCB coil.

TABLE III
SAMPLE PREPARATION

Sample	Material	Defects	Physical test piece
#1	#45 steel	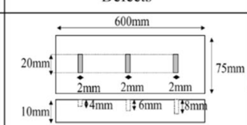	
#2	X80 carbon steel	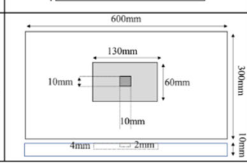	

The first layer and the third layer are hollow transmitters. The second layer and the fourth layer are differential receivers. The transmitter inductance bridge comprises two rectangular coils (L_1 and L_2), which were placed on the surface of the ferromagnetic sample sheet. The output of the inductance bridge circuit and the output of differential receiver were amplified using an instrument amplifier (AD8253). Finally, the amplitude and phase of the two channels were simultaneously acquired using an FPGA system in the integrated device. During the scanning operation, the signal could be seen in real time.

Table III shows the samples with two different materials and different kinds of defects. #1 is a 45-steel sample with a 10 mm thickness and defects at different depths (4, 6, and 8 mm). #2 is a carbon-steel sample with a composite defect comprising rectangular defects, and one of them is smaller and located inside the other. During the experimental process, the probe was fixed on an *XYZ* workbench, and all the defects were scanned at a consistent lift-off. Subsequently, the tests were repeated with varying lift-off ranges (0–10 mm). These materials were selected because they are commonly used in pipelines. Two different types of defect settings are used to simulate challenging scenarios in pipeline inspection, specifically addressing issues related to lift-off variation during depth changes and the presence of complex defects. In the case of the first type, both lift-off and depth variation can alter the amplitude of the voltage. It becomes challenging to confirm whether the signal is due to lift-off or a larger/smaller defect. Furthermore, distinguishing between multiple defects that are closely located, as in the case of #2, is also problematic.

B. Experimental Results of Two Samples

To address the challenges mentioned above, the proposed method for separating lift-off and defects is verified through experiments. Fig. 9(a) and (b) shows the results of the amplitude bridge output and transformer output when scanning three defects on the sample with varying lift-offs, respectively. Region I exhibits an edge effect due to the distance between defect and the edge being small. The probe passes through regions II–IV while detecting defects. The scale of output of bridge and transformer differs because the output of the bridge is the change in self-inductance under the primary magnetic field. The transformer captures the mutual inductance between the sample and the transmitter. As a result, the scale of output of the bridge is larger than the output of the transformer. The bridge output is more sensitive to the lift-off variation as the baseline of each output at different lift-off levels produces significant changes. In contrast, the voltage baseline of the transformer experiences little change but exhibits distinct variations when encountering defects. For comparison, the output of the bridge remains almost unchanged when passing over the defects. This observation importantly verifies that the proposed coil configuration with dual signal conditionings indeed possesses complementary characteristics for both lift-off and defect detection. Fig. 9(c) and (d) shows the results of amplitude bridge output and transformer output when scanning the composite defects on X80 carbon steel. Fig. 9(c) shows the output of the bridge, and it demonstrates that the baseline decreases as the lift-off distance increases. This pattern is similar to the results on #45 steel. However, there are two regions of slow change, labeled as regions I and II, which suggests that the bridge detected the edges of these composite defects. This indicates the number of defects, and their sizes can be preliminarily determined by combining both the bridge and transformer output. In addition, the baseline value of the bridge output serves as a characteristic feature to characterize lift-off.

Fig. 10 shows the comparison results between simulation results and the experiment for lift-off variation and defect detection. After fitting them to the same scale, both simulation and experimental results are consistent with each other.

C. Method for Lift-Off Estimation and Defect Evaluation

Considering the analysis above, the method for separating lift-off and defects is presented in Fig. 11. For lift-off distance, the baseline value is used to perform binomial fitting. Through solving the equation of the lift-off function, the lift-off can

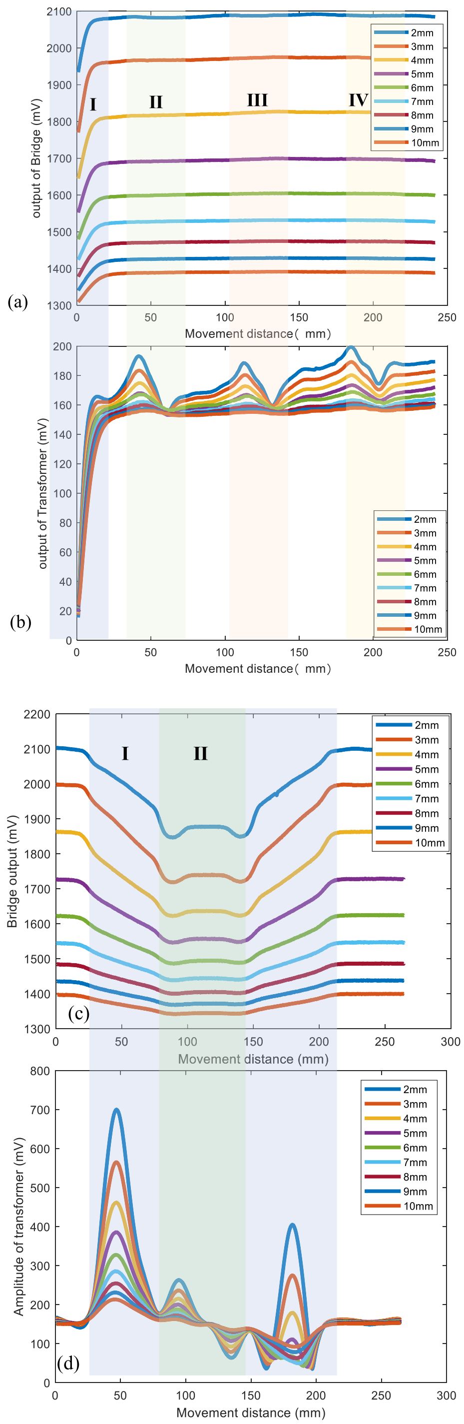

Fig. 9. Amplitude bridge output and transformer output. (a) Bridge output when scanning defects on sample #1 with varying lift-offs. (b) Transformer output when scanning defects on sample #1 with varying lift-offs. (c) Bridge output when scanning defects on sample #2 with varying lift-offs. (d) Transformer output when scanning defects on sample #2 with varying lift-offs.

be determined. Fig. 12 shows the lift-off functions on two samples, displaying the values at different lift-offs, as well as the absolute error and relative error acquired (presented in Table IV). The results demonstrate that the maximum relative error of the estimated value on these two samples is only, ±4%, with the minimum error ±0.3%. The possible sources of these small errors are primarily due to the challenge of accurately determining the zero position for the lift-off point.

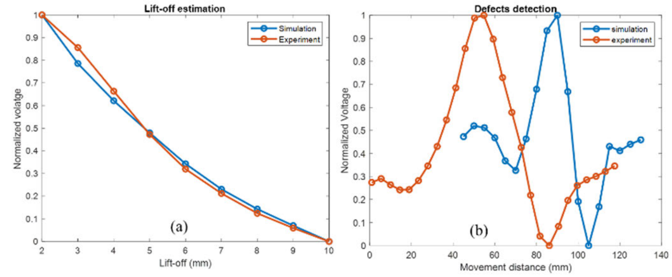

Fig. 10. Comparison between simulation and experimental results. (a) Lift-off measurement. (b) Defects detection.

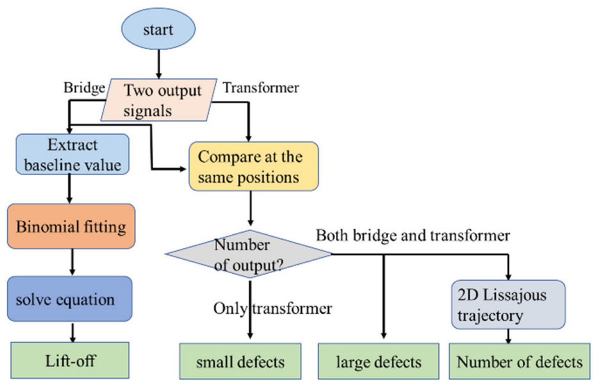

Fig. 11. Method for lift-off and defect separation.

In addition, it is difficult to guarantee that the probe and the surface of the test specimen are in a critical state under mechanical fixing. As a result, errors become more significant within a narrow range of lift-off distances (0–3 mm). For defect evaluation, two channels of output were combined. Due to their complementary characteristics, only the transformer output has distinct defect information, indicating that the defect is small compared with the size of the probe. If both channels of output have defect information, it means that the defect is larger than the size of the probe as the bridge shows two edges of defect. The experimental platform in [28] can also acquire the phase information. Then, the in-phase component I and quadrature component Q can be decomposed, namely

$$\begin{cases} I = \text{Amplitude} \times \cos(\text{phase}) \\ Q = \text{Amplitude} \times \sin(\text{phase}). \end{cases} \tag{13}$$

Subsequently, the 2-D Lissajous trajectory, typically used for defect identification, can be employed to determine the number of defects as shown in Fig. 13. In the figure, two "8" shape trajectories are presented to characterize this composite defect on carbon steel. Therefore, two defects can be easily distinguished.

The comparative analysis regarding the advantages of the multiparameters is presented in Table V. From the #45 steel results, we only get information about lift-off as the response of defects is too small to determine their presence. If we only consider the results of the transformer, it clearly indicates the existence of three defects, and it is difficult to evaluate whether the signal variation is affected by lift-off. With the proposed multiparameter method, both lift-off information and defect information can be easily obtained. Based on the

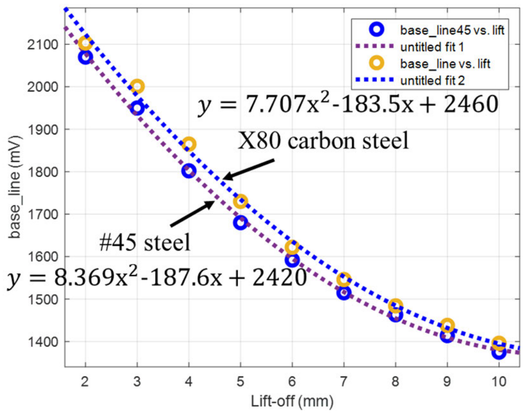

Fig. 12. Lift-off function on two tested samples.

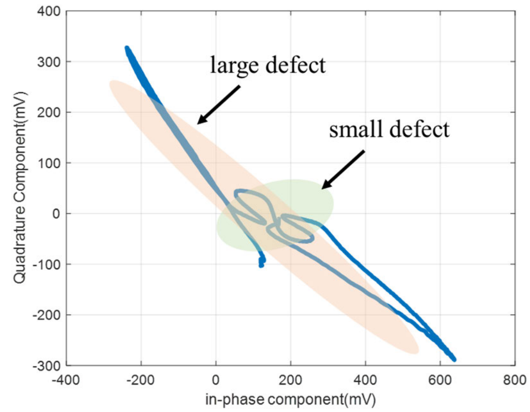

Fig. 13. Two-dimensional trajectory of in-phase and quadrature component.

TABLE IV
LIFT-OFF ESTIMATION

Lift-off (mm)	Estimation (mm)	absolute error	relative error
#45 steel lift-off estimation			
2	2.0590	0.0590	2.95%
3	2.8737	-0.1261	4.20%
4	4.0125	0.0125	0.30%
5	5.1090	0.1090	0.22%
6	6.0424	0.0424	0.07%
7	7.0268	0.0680	0.09%
8	7.8510	-0.1490	1.86%
9	8.8811	-0.1189	1.3%
10	10.3395	0.3395	3.40%
X80 carbon steel lift-off estimation			
Lift-off (mm)	Estimation (mm)	absolute error	relative error
2	2.1374	0.0910	4.50%
3	2.8617	-0.1383	4.61%
4	3.8723	-0.1277	3.19%
5	5.0488	0.0488	0.98%
6	6.1610	0.1610	2.68%
7	7.0954	0.0954	1.36%
8	8.0208	0.0208	0.26%
9	8.8854	-0.1146	1.27%
10	9.9898	-0.0102	0.10%

TABLE V
COMPARATIVE ANALYSIS

Signal conditionings	Lift-off	Defect	
#45 steel			
		size	number
Only Bridge	✓	×	×
Only Transformer	N	N	×
Both	✓	✓	✓
X80 carbon steel			
Signal conditionings	Lift-off	Defect	
		size	number
Only Bridge	✓	✓	✓
Only Transformer	N	✓	×
Both	✓	✓	✓

× indicates can be determined or not, N indicates uncertain

analysis above, it is possible to preliminarily classify the size of defects. Similarly, from the X80 carbon-steel results, we can evaluate both lift-off and defect information since the defects are large enough. For the results of the transformer, we can only speculate, based on the signal, that it is a large defect, whereas we cannot determine the information about lift-off or number of defects. In this scenario, we can gather information from the dual signal conditioning. These two complementary detection modes enhance the ability to consider multifactors in complex measurement environments and improve quantitative reliability, particularly in pipeline inspection. In fact, during pipeline inspection, defects are affected by multiple factors, making it difficult to determine whether the signal size is caused by lift-off or changes in the size of defects during the quantification process. In addition, defects in real environment have complex causes, with a wide range of defect types. Therefore, the proposed method can effectively assist in determining whether it is a single large defect or a corrosion group formed by multiple defects.

V. CONCLUSION AND FUTURE WORK

This article for the first time proposed a common-differential coils design with a dual signal conditioning platform to achieve lift-off estimation and defect separation. Specifically, a common-mode coil with a bridge circuit is designed for lift-off measurement and a differential transformer is used for defect detection. Through extracting the baseline value of the bridge output with binomial regression analysis, a functional relationship with lift-off can be established for lift-off inversion. Through combining the comprehensive analysis of the bridge and transformer output, the size of defects can be preliminarily estimated. In addition, the 2-D trajectory of in-phase and quadrature component was decomposed from the amplitude and phase. It can be used to preliminarily distinguish the number of defects. The lift-off distance estimation was achieved with ±4% maximum relative error in the 10-mm lift-off range and the minimum defect detected is 20 × 2 × 4 mm. In this way, multifactor judgment was increased and the quantitative reliability was improved due to two complementary detection modes in complex measurement environments such as pipeline inspection.

Future work will now concentrate on multiparameters for lift-off compensation and defect qualification based on these dual signal conditionings. In addition, a generalized lift-off model without influences on material for lift-off estimation is necessary. In addition, the speed effect and the possibility of industrial applications will be considered further. In addition to an ac bridge and transformer, the potential of other combination of signal conditioning with mutiparameters measurement will be studied as well, such as LC resonator, LR, or LDC.

References

[1] A. Sophian, G. Tian, and M. Fan, "Pulsed eddy current non-destructive testing and evaluation: A review," *Chin. J. Mech. Eng.*, vol. 30, no. 3, pp. 500–514, May 2017, doi: 10.1007/s10033-017-0122-4.

[2] X. Cheng, G. Ma, Z. Wu, H. Zu, and X. Hu, "Automatic defect depth estimation for ultrasonic testing in carbon fiber reinforced composites using deep learning," *NDT E Int.*, vol. 135, Apr. 2023, Art. no. 102804, doi: 10.1016/j.ndteint.2023.102804.

[3] H. Song, Q. Xiao, G. Wang, J. Zhang, and W. Hu, "A composite approach of electromagnetic acoustic transducer and eddy current for inner and outer corrosion defects detection," *IEEE Trans. Instrum. Meas.*, vol. 72, pp. 1–11, 2023, doi: 10.1109/TIM.2023.3238689.

[4] R. Wang, H. Yu, J. Tang, B. Feng, Y. Kang, and K. Song, "Optimal design of iron-cored coil sensor in magnetic flux leakage detection of thick-walled steel pipe," *Meas. Sci. Technol.*, vol. 34, no. 8, Aug. 2023, Art. no. 085123, doi: 10.1088/1361-6501/acd39c.

[5] A. N. Abdalla, M. A. Faraj, F. Samsuri, D. Rifai, K. Ali, and Y. Al-Douri, "Challenges in improving the performance of eddy current testing: Review," *Meas. Control*, vol. 52, nos. 1–2, pp. 46–64, Jan. 2019, doi: 10.1177/0020294018801382.

[6] A. Sophian, G. Y. Tian, D. Taylor, and J. Rudlin, "Electromagnetic and eddy current NDT: A review," *Insight*, vol. 43, no. 5, pp. 302–306, 2001.

[7] A. S. Repelianto and N. Kasai, "The improvement of flaw detection by the configuration of uniform eddy current probes," *Sensors*, vol. 19, no. 2, p. 397, Jan. 2019, doi: 10.3390/s19020397.

[8] Z. Yu, F. Yang, Y. Fu, and W. Huang, "Investigation of focusing properties of probes for pulsed eddy current testing," *IEEE Sensors J.*, vol. 21, no. 23, pp. 26830–26838, Dec. 2021, doi: 10.1109/JSEN.2021.3121147.

[9] L. Q. Trung, N. Kasai, K. Sekino, and S. Miyazaki, "Eddy current convergence probes with self-differential and self-nulling characteristics for detecting cracks in conductive materials," *Sens. Actuators A, Phys.*, vol. 349, Jan. 2023, Art. no. 114084, doi: 10.1016/j.sna.2022.114084.

[10] R. J. Ditchburn and S. K. Burke, "Planar rectangular spiral coils in eddy-current non-destructive inspection," *NDT E Int.*, vol. 38, no. 8, pp. 690–700, Dec. 2005, doi: 10.1016/j.ndteint.2005.04.001.

[11] K. R. Sandra, A. S. A. Kumar, B. George, and V. J. Kumar, "A linear differential inductive displacement sensor with dual planar coils," *IEEE Sensors J.*, vol. 19, no. 2, pp. 457–464, Jan. 2019, doi: 10.1109/JSEN.2018.2877209.

[12] Z. Xu, X. Wang, and Y. Deng, "Rotating focused field eddy-current sensing for arbitrary orientation defects detection in carbon steel," *Sensors*, vol. 20, no. 8, p. 2345, Apr. 2020.

[13] N. M. Rodrigues, L. S. Rosado, and P. M. Ramos, "A portable embedded contactless system for the measurement of metallic material conductivity and lift-off," *Measurement*, vol. 111, pp. 441–450, Dec. 2017, doi: 10.1016/j.measurement.2017.05.002.

[14] M. A. Machado, K.-N. Antin, L. S. Rosado, P. Vilaça, and T. G. Santos, "Contactless high-speed eddy current inspection of unidirectional carbon fiber reinforced polymer," *Compos. B, Eng.*, vol. 168, pp. 226–235, Jul. 2019, doi: 10.1016/j.compositesb.2018.12.021.

[15] C. Ye, N. Zhang, L. Peng, and Y. Tao, "Flexible array probe with in-plane differential multichannels for inspection of microdefects on curved surface," *IEEE Trans. Ind. Electron.*, vol. 69, no. 1, pp. 900–910, Jan. 2022, doi: 10.1109/TIE.2021.3050376.

[16] D. I. Ona, G. Y. Tian, R. Sutthaweekul, and S. M. Naqvi, "Design and optimisation of mutual inductance based pulsed eddy current probe," *Measurement*, vol. 144, pp. 402–409, Oct. 2019, doi: 10.1016/j.measurement.2019.04.091.

[17] H. Hoshikawa, K. Koyama, and H. Karasawa, "A new eddy current surface probe without lift-off noise," in *Proc. 10th APCNDT*, 2001, pp. 275–8575.

[18] L. Huang, C. Liao, X. Song, T. Chen, X. Zhang, and Z. Deng, "Research on detection mechanism of weld defects of carbon steel plate based on orthogonal axial eddy current probe," *Sensors*, vol. 20, no. 19, p. 5515, Sep. 2020, doi: 10.3390/s20195515.

[19] K. Chen, B. Gao, G. Y. Tian, Y. Yang, C. Yang, and Q. Ma, "Differential coupling double-layer coil for eddy current testing with high lift-off," *IEEE Sensors J.*, vol. 21, no. 16, pp. 18146–18155, Aug. 2021, doi: 10.1109/JSEN.2021.3076880.

[20] J. Zhao, W. Li, X. Yuan, X. Yin, Q. Chen, and J. Zhao, "Lift-off point of intersection for eliminating Lift-off noise in alternating current field measurement," *IEEE Trans. Instrum. Meas.*, vol. 72, pp. 1–9, 2023, doi: 10.1109/TIM.2023.3285996.

[21] X. Li, G. Tian, K. Li, H. Wang, and Q. Zhang, "Differential ECT probe design and investigation for detection of rolling contact fatigue cracks with different orientations," *IEEE Sensors J.*, vol. 22, no. 12, pp. 11615–11625, Jun. 2022, doi: 10.1109/JSEN.2022.3170598.

[22] J. Li, X. Wu, Q. Zhang, and P. Sun, "Measurement of lift-off using the relative variation of magnetic flux in pulsed eddy current testing," *NDT E Int.*, vol. 75, pp. 57–64, Oct. 2015, doi: 10.1016/j.ndteint.2015.06.008.

[23] W. Yin and K. Xu, "A novel triple-coil electromagnetic sensor for thickness measurement immune to lift-off variations," *IEEE Trans. Instrum. Meas.*, vol. 65, no. 1, pp. 164–169, Jan. 2016, doi: 10.1109/TIM.2015.2479106.

[24] P. Huang, Z. Li, J. Long, L. Xu, and Y. Xie, "Measurement of lift-off distance and thickness of nonmagnetic metallic plate using pulsed eddy current testing," *IEEE Trans. Instrum. Meas.*, vol. 72, pp. 1–10, 2023, doi: 10.1109/TIM.2023.3285918.

[25] M. Lu, X. Meng, R. Huang, L. Chen, A. Peyton, and W. Yin, "Measuring lift-off distance and electromagnetic property of metal using dual-frequency linearity feature," *IEEE Trans. Instrum. Meas.*, vol. 70, pp. 1–9, 2021, doi: 10.1109/TIM.2020.3029348.

[26] W. Chen and D. Wu, "Resistance-frequency eddy current method for electrical conductivity measurement," *Measurement*, vol. 209, Mar. 2023, Art. no. 112501, doi: 10.1016/j.measurement.2023.112501.

[27] G. Tian, C. Yang, X. Lu, Z. Wang, Z. Liang, and X. Li, "Inductance-to-digital converters (LDC) based integrative multi-parameter eddy current testing sensors for NDT&E," *NDT E Int.*, vol. 138, Sep. 2023, Art. no. 102888, doi: 10.1016/j.ndteint.2023.102888.

[28] S. Sreevatsan and B. George, "Simultaneous detection of defect and lift-off using a modified pulsed eddy current probe," *IEEE Sensors J.*, vol. 20, no. 4, pp. 2156–2163, Feb. 2020, doi: 10.1109/JSEN.2019.2949340.

[29] P. Huang et al., "A novel eddy current method for defect detection immune to lift-off," *IEEE Trans. Instrum. Meas.*, vol. 71, pp. 1–13, 2022, doi: 10.1109/TIM.2022.3199272.

[30] T. Zhu et al., "A dual mode nondestructive evaluation sensor with simultaneous inductive and capacitive outputs," *IEEE Sensors J.*, vol. 23, no. 6, pp. 6214–6224, Mar. 2023, doi: 10.1109/JSEN.2023.3241923.

[31] Q. Ma, G. Y. Tian, B. Gao, X. Zhao, G. Ru, and H. Li, "Lift-off suppression based on combination of bridge and transformer signal conditionings of eddy current testing," *NDT E Int.*, vol. 132, Dec. 2022, Art. no. 102724, doi: 10.1016/j.ndteint.2022.102724.

[32] J. Yin, G. Zhao, Z. Feng, and J. Ni, "A novel dual-differential edge sensor based on the eddy current effect," *IEEE Sensors J.*, vol. 23, no. 6, pp. 6129–6138, Mar. 2023, doi: 10.1109/JSEN.2023.3240175.

[33] A. Ulla Khan, T. Islam, and J. Akhtar, "An oscillator-based active bridge circuit for interfacing capacitive sensors with microcontroller compatibility," *IEEE Trans. Instrum. Meas.*, vol. 65, no. 11, pp. 2560–2568, Nov. 2016, doi: 10.1109/TIM.2016.2581519.

[34] H. Wang, B. Ju, W. Li, and Z. Feng, "Ultrastable eddy current displacement sensor working in harsh temperature environments with comprehensive self-temperature compensation," *Sens. Actuators A, Phys.*, vol. 211, pp. 98–104, May 2014, doi: 10.1016/j.sna.2014.03.008.

Qiuping Ma received the B.Sc. degree in electronic information engineering from Sichuan Normal University, Chengdu, China, in 2017. She is currently pursuing the Ph.D. degree in electromagnetic nondestructive evaluation with the University of Electronic Science and Technology of China, Chengdu.

Her research interests include eddy current sensors design, simulation, pipeline inspection, and multiphysics multiparameters measurement.

Guiyun Tian (Senior Member, IEEE) received the B.Sc. degree in metrology and instrumentation and the M.Sc. degree in precision engineering from the University of Sichuan, Chengdu, China, in 1985 and 1988, respectively, and the Ph.D. degree from the University of Derby, Derby, U.K., in 1998.

From 2000 to 2006, he was a Lecturer, a Senior Lecturer, a Reader, a Professor, and the Head of the Group of Systems Engineering, University of Huddersfield, Huddersfield, U.K. Since 2007, he has been with Newcastle University, Newcastle upon Tyne, U.K.

Bin Gao (Senior Member, IEEE) received the B.Sc. degree in communications and signal processing from Southwest Jiao Tong University, Chengdu, China, in 2005, and the M.Sc. (Hons.) degree in communications and signal processing and the Ph.D. degree from Newcastle University, Newcastle upon Tyne, U.K., in 2006 and 2011, respectively.

From 2011 to 2013, he worked as a Research Associate with Newcastle University, on wearable acoustic sensor technology. He is currently a Professor with the School of Automation Engineering, University of Electronic Science and Technology of China (UESTC), Chengdu. His research interests include electromagnetic and thermography sensing, machine learning, and nondestructive testing and evaluation, where he actively publishes in these areas.

Dr. Gao is also a very active reviewer for many international journals and long-standing conferences.

Mark Robinson is a Professor of Rail Systems Engineering with the School of Engineering, Newcastle University, Newcastle upon Tyne, U.K., and a Technologies Lead with the Newcastle University Centre of Excellence for Mobility and Transport, Newcastle upon Tyne. He is also the Director of the Newcastle Centre for Rail Research (NewRail) and a Fellow of the Institute of Materials, Minerals and Mining (FIMMM), a Chartered Engineer (CEng), and a Chartered Scientist (CSci). His main research interests include asset management, infrastructure and rail vehicle maintenance, railway technology, inspection and monitoring techniques, the development and application of lightweight materials for vehicles, and composite structures. He is a specialist in infrastructure and rail vehicle inspection and monitoring and uses this expertise for consultancy purposes.

Mr. Robinson is an Academic Member of the European Rail Research Advisory Council (ERRAC). He has won awards for vehicle joining technologies and use of composites for lightweighting of rail vehicles. He is the Vice Chairperson of the Union of International Railway's (UIC) International Rail Research Board (IRRB) responsible for Working Group 5—International Rail Academic Network. He is the past President of the European Conference of Transport Research Institute (ECTRI).

Changrong Yang received the B.Sc. degree in measurement and control technology and instrument from Southwest Petroleum University, Chengdu, China, in 2017, and the M.Sc. degree in instrument science and technology from the University of Electronic Science and Technology of China, Chengdu, in 2020. He is currently pursuing the Ph.D. degree in electrical and electronic engineering with the School of Engineering, Newcastle University, Newcastle upon Tyne, U.K.

His research interests include wireless LC resonant sensing for force measurement.

Emmanuel Tashiwa Ibrahim received the B.Eng. degree in electrical and electronic engineering from the Federal University of Technology, Yola, Adamawa, Nigeria, in 2004, and the M.Eng. degree in electronic and telecommunication engineering from the University of Benin, Benin, Edo, Nigeria, in 2007. He is currently pursuing the Ph.D. degree in electrical and electronic engineering with the School of Engineering, Newcastle University, Newcastle upon Tyne, U.K.

He joined the Department of Electrical and Electronic Engineering, University of Abuja, Abuja, Nigeria, in 2009, as an Academic Staff Member. His primary research interests include electromagnetic sensing for nondestructive testing and evaluation (NDT&E).